# Liquid-to-Solid Phase Transition of a 1,3-Dimethylimidazolium Chloride Ionic Liquid Monolayer Confined between Graphite Walls

**Maolin Sha,[†,‡] Guozhong Wu,[*,†] Haiping Fang,[*,†] Guanglai Zhu,[†,‡] and Yusheng Liu[†,‡]**

*Shanghai Institute of Applied Physics, Chinese Academy of Sciences, Shanghai 201800, P.B. Box 800-204, China, Graduate School of the Chinese Academy of Sciences, Beijing 10039, People's Republic of China*

*Received: September 6, 2008*

Molecular dynamics simulations were performed to study the phase behavior of a monolayer of room temperature ionic liquid 1,3-dimethylimidazolium chloride ([Dmim][Cl]) confined between two graphite walls at 425 K. These simulations predict a first-order freezing transition from a liquid monolayer to a solid monolayer induced by varying the distance between the parallel graphite walls ($H = \sim 0.65-0.95$ nm). The resulting monolayer solid consisting of a hydrogen-bonded network structure is very different from bulk crystalline [Dmim][Cl]. The phase transition can be induced only at a molecular surface density of $\rho = 1.9/\text{nm}^2$.

Room-temperature ionic liquids (ILs) have received much attention in recent years due to their importance in a broad range of applications,[1,2] yet little is understood about the microstructure and phase transition of ILs in confined systems. An understanding of the microstructure and freezing processes of ILs in confined systems is of practical importance in lubrication, adhesion, and the fabrication of solar cells or IL/nanomaterial composites, in which ILs are in contact with solid surfaces or under confinement. In general, the reduction of the liquid film thickness to fewer than 4−6 molecular layers will promote solidification. This results from the characteristic transverse density profile of thin films, which can induce lateral ordering and lead to freezing. It has been demonstrated that water confined in nanospaces exhibits anomalous phase behaviors, which are typically illustrated experimentally or via MD simulation.[3−9] For example, Koga et al.[3,4] found the existence of a variety of new ice phases between two parallel walls, implying a transition from liquid water to new ice configurations. Some evidence has indicated a possible liquid−solid phase transition for ionic liquids in confined systems.[10] Several reports have also revealed the astonishing property of melting point depression of 1,3-dialkylimidazolium-based ionic liquids confined to nanospaces, which was discovered utilizing differential scanning thermal calorimetry.[11,12] However, the phase behavior of ionic liquids confined to nanospaces remains largely unexplored. Here, we report the first simulation results of a liquid−solid freezing transition of 1,3-dimethylimidazolium chloride ([Dmim][Cl]) ionic liquid between two parallel graphite walls. This result is also of importance to the understanding of interfacial interactions between ionic liquids and carbon nanotubes because ionic liquid is found to disperse uniformly on the surface of single-walled carbon nanotubes via simple mulling.[13]

We utilized molecular dynamics (MD) simulations to investigate the freezing of a [Dmim][Cl] monolayer. The melting point of the bulky [Dmim][Cl] at ambient pressure (0.1 MPa) was recently estimated to be ×399 K.[14] Hence, the simulations were performed at a fixed temperature at 425 K, using Gromacs 3.2.[15] A system of a fixed number ($N$) of 60 [Dmim][Cl] molecules was placed between two graphite walls fixed in a space. The [Dmim][Cl] molecule, as shown in Figure 1a, was treated as a systematic all-atom force field developed by Lopes et al.[16] The graphite wall is constructed from 22 × 13 elementary

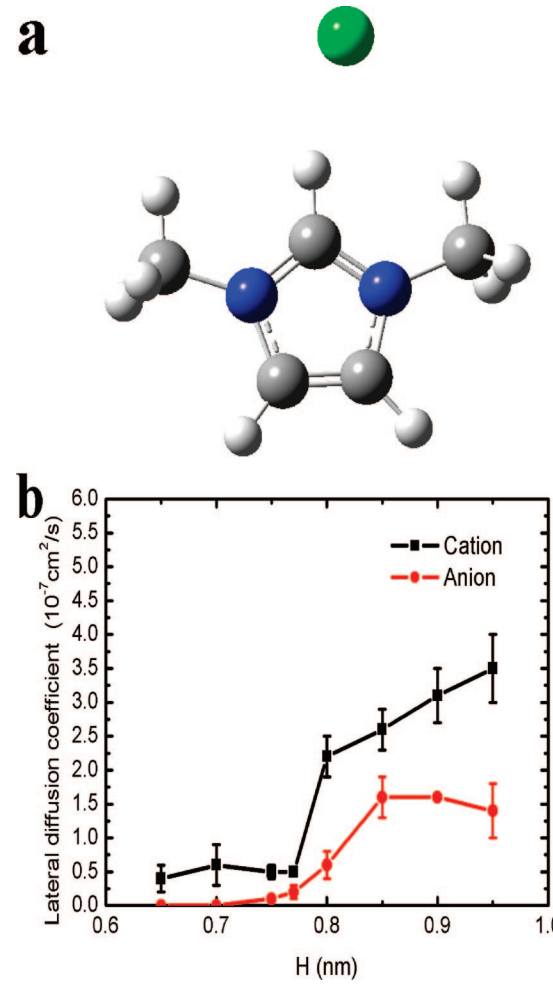


**Figure 1.** (a) Scheme of [Dmim][Cl] molecular configuration. (b) Lateral diffusion coefficients as a function of the distance between the confining graphite walls.

* To whom correspondence should be addressed. E-mail: wuguozhong@sinap.ac.cn; fanghaiping@sinap.ac.cn.
† Shanghai Institute of Applied Physics.
‡ Graduate School of the Chinese Academy of Sciences.

10.1021/jp8079183 CCC: $40.75 
Published on Web 10/31/2008

cells, leading to a surface dimensions $l_x = 56.56$ Å and $l_y = 55.38$ Å. The $[Dmim]^+$−wall interactions were represented by a 6−12 Lennard−Jones potential with the same parameters used in our previous work.[17] The anionic chloride atoms were also modeled using an OPLS-AA force field.[18] The cross interactions were computed according to the conventional combination rule: $\sigma_{ij} = (\sigma_i\sigma_j)^{1/2}$ and $\varepsilon_{ij} = (\varepsilon_i\varepsilon_j)^{1/2}$ for OPLS-AA in Gromacs.

A first set of simulations was run at constant wall distance, $H$, with $T = 425$ K. Periodic boundary conditions were applied in the $x$ and $y$ directions. In all the simulations, bond length was constrained with LINCS algorithm. Cutoff of Lennard−Jones interactions was taken at 12 Å. The long-range coulomb interactions were handled by PME with a cutoff of 15 Å and a grid spacing of 1.2 Å. The berendsen thermostat was used to mimick weak coupling at 425 K; cations and anions were separated into two heat baths with temperature coupling constants of 0.1 ps. Since the cation size of [Dmim][Cl] is about 0.6 nm, the initial configuration is prepared by taking a thin out-of-order layer ($H = 0.65$ nm) of [Dmim][Cl]. All the systems were run 1 ns at 1200 K and then annealed from 1200 to 425 K in three stages: 1 ns at 800 K, 1 ns at 600 K, and 1 ns at 425 K. At each thermodynamic point (achieved by a sequential increase in $H$) the system was again equilibrated for 5 ns, and data was collected for the additional 3 ns.

Figure 1b shows the cation and anion lateral diffusion coefficients for wall separations in the range $0.65 \text{ nm} \le H \le 1.0$ nm. For wall distances in the range $0.8 \text{ nm} < H < 0.95$ nm, the [Dmim][Cl] is a liquid monolayer, as indicated by the large diffusion coefficient. At $H < 0.8$ nm, the liquid monolayer transforms into a frozen state, as indicated by a value of nearly 0 for the lateral diffusion coefficient of the anions. At $H = 0.95$ nm, the liquid monolayer transforms into a bilayer (see Figure 2c). This liquid−solid transition trend is similar to that reported by Gao et al.[9] for an atomic fluid between corrugated walls, where evidence of a confinement-induced transition to a solidlike phase was observed. The structure of the [Dmim][Cl] solid monolayer obtained for a wall distance of $H = 0.7$ nm is shown in Figure 2a. The distance is close to the pore size in typical commercial activated carbons. Figure 2b shows inherent structures of the liquid monolayer confined between walls ($H = 0.9$ nm). In the solid monolayer, the imidazolium ring of cations is nearly planar, and the anion is horizontally close to it. However, these features are not observed in the bulk liquid phase. More crucial is the difference in the hydrogen-bond network structure. In the new solid monolayer, each cation is surrounded by four near-neighbor anions, while each anion is also encircled by four neighbor cations. This solid phase monolayer has a local network structure very different from that of bulk crystalline [Dmim][Cl],[19] in which each anion is pinched between two coplanar cations. In the liquid monolayer and bilayer, the hydrogen bond network structure is partially breached, and the rings of cations are no longer entirely planar. In the bulk liquid, the most probable distribution of the anions around the cations is a 3-dimensional structure. [20−22]

The configuration change induced by changes in the wall distance can also be seen in the 2-dimensional radial distribution function (Figure 3). There is a clear long-range order for the solid monolayer ($H = 0.70$ nm) in both cation−anion and anion−anion distributions. As $H$ exceeds the transition point at 0.8 nm, the peak height and the refined structure start to fade away. If $H$ is increased continuously, as studied by Kohanoff et al.,[23] the IL will retain a liquid behavior rather than transition to a solidlike structure. The origin of this phenomenon is a collective effect, including a density effect and a unique interaction between [Dmim][Cl] molecules and the graphite wall. The plots corresponding to $H = 0.9$ nm still retain partial long-

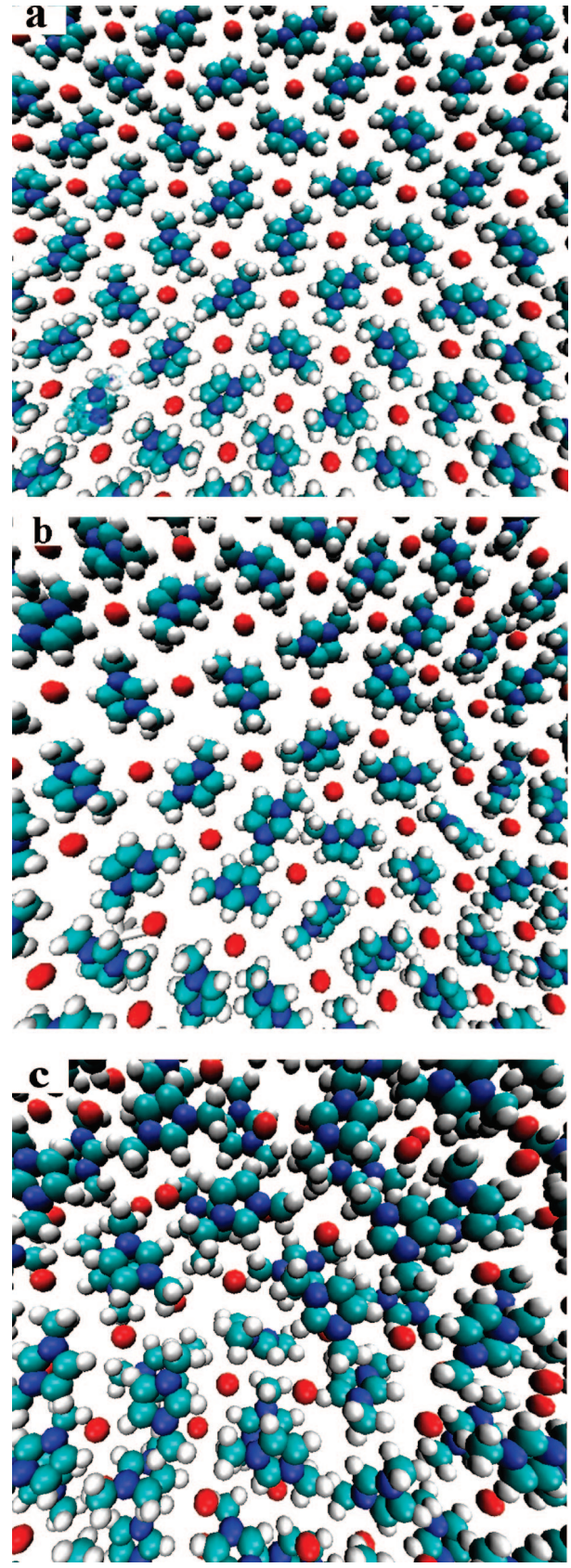


**Figure 2.** Structure of the confined [Dmim][Cl] in solid and liquid states. (a) A solid monolayer, $H = 0.70$ nm. (b) A liquid monolayer, $H = 0.9$ nm. (c) A liquid bilayer, $H = 0.95$ nm. Anions are depicted in red.

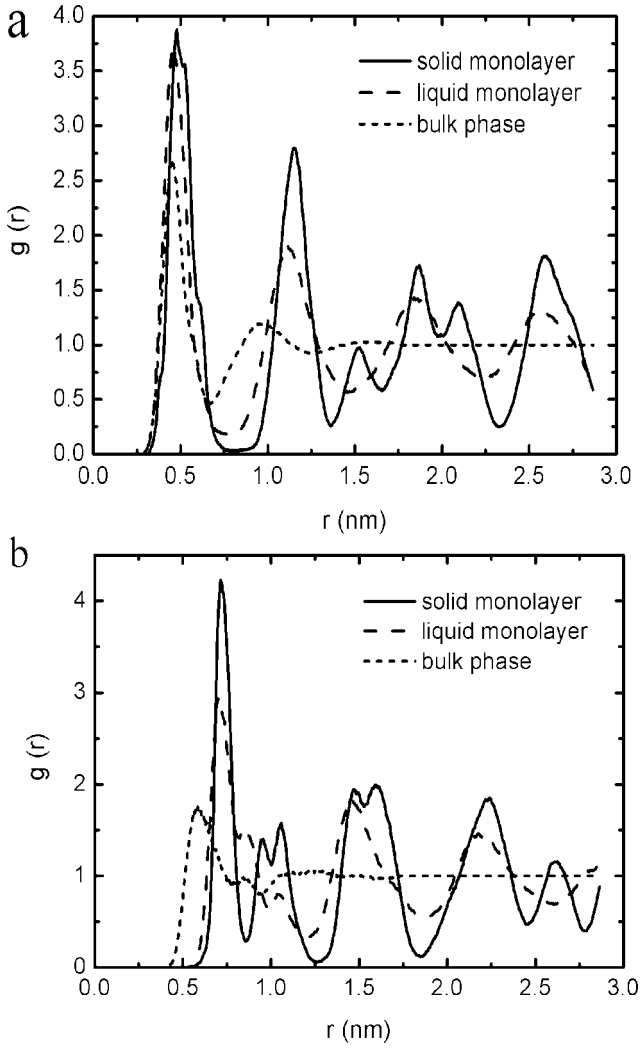


**Figure 3.** The mass-center radial distribution functions of the cation−anion and the anion−anion in bulky phase, monolayer of liquid ($H = 0.9$ nm) and monolayer of solid ($H = 0.7$ nm). (a) A cation−anion distribution. (b) An anion−anion distribution.

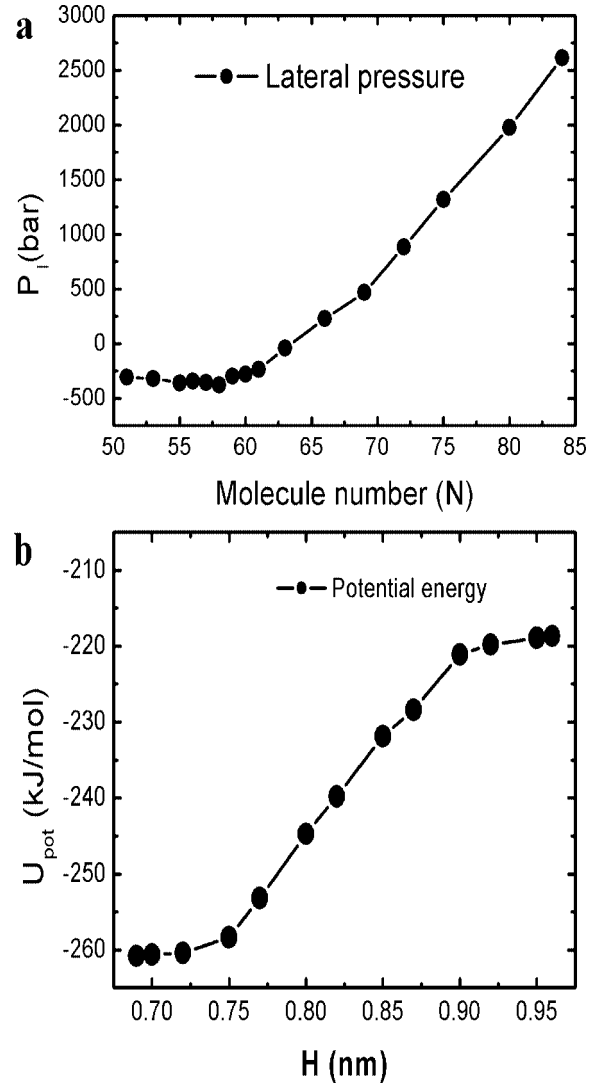


**Figure 4.** (a) The isotherms of the lateral pressure as a function of $N$. Simulations at constant molecule number, N; wall area, A; and wall distance, $H = 0.75$ nm. (b) The distance dependence of potential energies at 425 K. The potential energy consists of the cation−cation, the cation−anion, the anion−anion intermolecular interactions and the cation−walls, the anion−walls interactions.

range order, in contrast to the disorder of the bulk liquid phase. Such partial order arises from the preferred orientations of [Dmim][Cl] at the solid surface. Similar results have been found in our previous simulation and many other reports.[17,23,24] Under confinement, the ions can assemble into a contact layer with an orientational preference induced by the solid surface. Further analysis of the cation−anion pairs correlation function in Figure 3a reveals that monolayer configurations ($H = 0.7$ and 0.9 nm) exhibit an obvious shift in the second shell of the nearest neighbors relative to the behavior of the bulk phase. The confinement forces the anions of the monolayer to approach the cations in a 2-dimensional planar structure rather than a 3-dimensional structure, as in the bulk phase. This is clearly revealed by the anion−anion pair correlation function in Figure 3b. In contrast to monolayer configurations, there is an evident shift in the first shell of nearest neighbors for the bulk phase. We also note that the anion−anion distribution for the solid monolayer ($H = 0.7$ nm) in Figure 2b exhibits a clear second shell maximum at around $r = 1.0$ nm. With the transition from the liquid monolayer to the solid monolayer, the shell number both in cation−anion and anion−anion distributions becomes much larger. However, the freezing transition occurs at a temperature ($T = 425$ K) well above the freezing temperature of a bulky [Dmim][Cl] liquid ($T = 399$ K).

It is important to note that recent MD simulations of the same ionic liquid confined between hydrophobic walls indicated no "hardening" or transition to a solidlike phase structure,[23] but only down to a wall distance of 2.5 nm. Our results clearly suggest that the wall distance plays a crucial role in the phase transition. Like an ice monolayer confined between walls,[4,5] the molecule area density ($\rho = N/l_x l_y$) of [Dmim][Cl] is another important factor. Figure 4a shows an isotherm of the lateral pressure as a function of molecule number $N$, in a second set of simulations at constant $N$, $A$, $T$, and $H$. The initial configuration was an out-of-order monolayer of 84 [Dmim][Cl] molecules at a wall distance of $H = 0.75$ nm. The molecule number of the system was then decreased in steps and simulated for time periods equal to the first set of simulations. The change in $N$ reflects the change in surface density, $\rho$, since the area of the graphite wall remains unchanged in the simulation. As the molecule number is decreased, the lateral pressure of the monolayer liquid decreases to a lower value. For $N \leq 60$, the phase is a solid monolayer with the same degree of ordering as was observed in the preceding simulations at constant lateral pressure. The freezing transition is very sensitive to the value

of $\rho$. In our simulation, the phase transition can be induced at $\rho = 1.9/\text{nm}^2$. If the surface density exceeds this value, a solid monolayer will not be formed. Meanwhile, we also studied the vertical pressure effect on the solid monolayer. It was interesting to note that the formed solid monolayer is not dependent on the vertical pressure. Actually, between the distance 0.65 nm $< H <$ 0.75 nm (the distance can induce the phase transition of the solid monolayer), there is always a smaller pressure value, from 700 to −200 bar. The interaction energy between the ionic liquid and the walls is about −62 kJ/mol at a distance of 0.7 nm. Hence, the above results imply that the configurational effect and the attraction interaction between the ionic liquid and the walls collectively induce the solid monolayer. Figure 4b shows the wall distance dependence of potential energy at 425 K. As the $H$ is decreased, the potential energy suddenly drops by about 40 kJ/mol within a 0.15 nm range (from 0.90 to 0.75 nm). Moreover, the lateral diffusion coefficients also decreased steeply with H in this region (Figure 1b). For $H \leq 0.75$ nm, the phase is a solid monolayer, as shown in Figure 2b. Both the distance dependences of the diffusion coefficient and the potential energy indicate a strong first-order phase transition in confined [Dmim][Cl].

In summary, a first-order liquid-to-solid phase transition of ionic liquid [Dmim][Cl] confined between graphite walls was observed using molecular dynamics simulations. The behavior of a solid monolayer is very different from that of the bulk crystalline [Dmim][Cl]. These results are helpful for the understanding of microstructures of ionic liquids in nanostructured confinement as well as the thermodynamic mechanism of liquid-to-solid phase transition.

**Acknowledgment.** This work was supported by the National Science Foundations of China (20573130 and 20673137), Shanghai Municipal Committee of Science and Technology, and Shanghai Supercomputer Center of China. We thank Prof. J. Hu and Dr. C. L. Wang for their valuable discussions.

## References and Notes

(1) Welton, T. *Chem. Rev.* **1999**, *99*, 2071.
(2) Rogers, R. D.; Seddon, K. R. *Science* **2003**, *302*, 792.
(3) Koga, K.; Tanaka, H.; Zeng, X. C. *Nature* **2000**, *408*, 564.
(4) Koga, K.; Zeng, X. C.; Tanaka, H. *Phys. Rev.Lett.* **1997**, *79*, 5262.
(5) (a) Zangi, R.; Mark, A. E. *Phys. Rev. Lett.* **2003**, *91*, 025502. (b) Zangi, R.; Mark, A. E. *J. Chem. Phys.* **2003**, *119*, 1694.
(6) Leng, Y. S.; Cummings, P. T. *Phys. Rev. Lett.* **2005**, *94*, 026101.
(7) Zhu, Y. X.; Granick, S. *Phys. Rev. Lett.* **2001**, *87*, 096104.
(8) Major, R. C.; Houston, J. E.; McGrath, M. J.; Siepmann, J. I.; Zhu, X. Y. *Phys. Rev. Lett.* **2006**, *96*, 177803.
(9) (a) Gao, J.; Luedtke, W. D.; Landman, U. *Phys. Rev. Lett.* **1997**, *79*, 705. (b) Gao, J.; Luedtke, W. D.; Landman, U. *J. Phys.Chem. B* **1997**, *101*, 4013.
(10) (a) Chen, S. M.; Wu, G. Z.; Sha, M. L.; Huang, S. R. *J. Am. Chem. Soc.* **2007**, *129*, 2416. (b) Liu, Y. D.; Zhang, Y.; Wu, G. Z.; Hu, J. *J. Am. Chem. Soc.* **2006**, *128*, 7456.
(11) Kanakubo, M.; Hiejima, Y.; Minami, K.; Aizawa, T.; Nanjo, H. *Chem. Commun.* **2006**, 1828.
(12) Néouze, M.; Bideau, J. L.; Gaveau, P.; Bellayer, S.; Vioux, A. *Chem. Mater.* **2006**, *18*, 3931.
(13) Fukushima, T.; Kosaka, A.; Ishimura, Y.; Yamamoto, T.; Takigawa, T.; Ishii, N.; Aida, T. *Science* **2003**, *300*, 2072–2074.
(14) Fannin, A. A.; Floreani, D. A.; King, L. A.; Landers, J. S.; Piersma, B. J.; Stech, D. J.; Vaughn, R. L.; Wilkes, J. S.; Williams, J. L. *J. Phys. Chem.* **1984**, *88*, 2614.
(15) Lindahl, E.; Hess, B.; Van der Spoel, D. J. *Mol. Mod.* **2001**, *7*, 306.
(16) Canongia Lopes, J. N.; Deschamps, J.; Pódua, A. A. H. *J. Phys. Chem. B* **2004**, *108*, 2038.
(17) Sha, M. L.; Zhang, F. C.; Wu, G. Z.; Fang, H. P.; Wang, C. L.; Chen, S. M.; Zhang, Y.; Hu, J. *J. Chem. Phys.* **2008**, *128*, 134504.
(18) Jorgensen, W. L.; Maxwell, D. S.; Tirado-Rives, J. *J. Am. Chem. Soc.* **1996**, *118*, 11225.
(19) Arduengo, A. J.; Dias, H. V. R.; Harlow, R. L.; Kline, M. *J. Am. Chem. Soc.* **1992**, *114*, 5530.
(20) Hanke, C. G.; Price, S. L.; Lynden-Bell, R. M. *Mol. Phys.* **2001**, *99*, 801.
(21) Bhargava, B. L.; Balasubramanian, S. *Chem. Phys. Lett.* **2006**, *417*, 486.
(22) Hardacre, C.; McMath, S E J.; Nieuwenhuyzen, M.; Bowron, D. T.; Soper, A. *J. Phys.: Condens. Matter* **2003**, *15*, 159.
(23) Pinilla, C.; Pópolo, M. G. D.; Lynden-Bell, R. M.; Kohanoff, J. *J. Phys. Chem. B* **2005**, *109*, 17922.
(24) (a) Atkin, R.; Warr, G. G. *J. Phys. Chem. C* **2007**, *111*, 5162. (b) Atkin, R.; Warr, G. G. *J. Am. Chem. Soc.* **2005**, *127*, 11940.

JP8079183